Geological Society of America Bulletin, published online on 21 October 2015 as doi:10.1130/B31294.1

A hot and high Eocene Sierra Nevada

Hari T. Mix[1,2,†], Daniel E. Ibarra[2], Andreas Mulch[3,4,5], Stephan A. Graham[6], and C. Page Chamberlain[2]
[1]*Department of Environmental Studies and Sciences, Santa Clara University, Santa Clara, California 95053, USA*
[2]*Department of Earth System Science, Stanford University, Stanford, California 94305, USA*
[3]*Senckenberg Biodiversity and Climate Research Centre (BiK-F), 60325 Frankfurt/Main, Germany*
[4]*Institut für Geowissenschaften, Goethe Universität Frankfurt, 60438 Frankfurt/Main, Germany*
[5]*Senckenberg Research Institutes and Natural History Museums, Senckenberganlage 25, 60325 Frankfurt/Main, Germany*
[6]*Department of Geological Sciences, Stanford University, Stanford, California 94305, USA*

ABSTRACT

Despite broad interest in determining the topographic and climatic histories of mountain ranges, the evolution of California's Sierra Nevada remains actively debated. Prior stable isotope–based studies of the Sierra Nevada have relied primarily on hydrogen isotopes in kaolinite, hydrated volcanic glass, and leaf *n*-alkanes. Here, we reconstruct the temperature and elevation of the early Eocene Sierra Nevada using the oxygen isotope composition of kaolinitized granite clasts from the ancestral Yuba and American Rivers that drained the windward (Pacific) flank of the Sierra Nevada. First, we evaluated the possible contributions of hydrogen isotope exchange in kaolinite by direct comparison with oxygen isotope measurements. Next, we utilized differences in the hydrogen and oxygen isotope fractionation in kaolinite to constrain early Eocene midlatitude weathering temperatures. Oxygen isotope geochemistry of in situ kaolinites indicates upstream (eastward) depletion of ^{18}O in the northern Sierra Nevada. The $\delta^{18}O$ values, ranging from 11.4‰ to 14.4‰ at the easternmost localities, correspond to paleoelevations as high as 2400 m when simulating the orographic precipitation of moisture from a Pacific source using Eocene boundary conditions. This result is consistent with prior hydrogen isotope studies of the northern Sierra, but oxygen isotope–based paleoelevation estimates are systematically ~500–1000 m higher than those from hydrogen-based estimates from the same samples. Kaolinite geothermometry from 16 samples produced early Eocene weathering temperatures of 13.0–36.7 °C, with an average of 23.2 ± 6.4 °C (1σ). These kaolinite temperature reconstructions are in general agreement with paleofloral and geochemical constraints from Eocene California localities and climate model simulations. Our results confirm prior hydrogen isotope–based paleoelevation estimates and further substantiate the existence of a hot and high Eocene Sierra Nevada.

INTRODUCTION

Earth's topography reflects the balance among tectonic, Earth surface, and climatic processes. As such, determining paleoelevation and paleoclimate histories of mountain belts provides insight into the evolution and multiple interactions of these processes (e.g., Chase et al., 1998; Blisniuk and Stern, 2005; Mulch and Chamberlain, 2007; Clark, 2007; Rowley and Garzione, 2007; Mix et al., 2011; Chamberlain et al., 2012). Stable isotope–based reconstructions provide one of the few methods that can be used to quantitatively reconstruct the evolution of topography in the world's largest mountain and plateau regions (e.g., Chamberlain et al., 1999; Garzione et al., 2000, 2008; Rowley et al., 2001; Mulch et al., 2004; Rowley and Currie, 2006; Rowley and Garzione, 2007; Lechler and Galewsky, 2013; Saylor and Horton, 2014). Stable isotope paleoaltimetry exploits systematic changes in the hydrogen or oxygen isotope ratios of meteoric water, which ultimately relate to changes in paleoelevation. This technique has been shown to reliably reconstruct past elevation histories in most of the world's large mountain ranges, including the Himalaya and Tibet (e.g., Garzione et al., 2000; Rowley and Currie, 2006; Gébelin et al., 2013), the Andes (e.g., Blisniuk and Stern, 2002; Garzione et al., 2006, 2008; Mulch et al., 2010; Canavan et al., 2014), the Southern Alps (Chamberlain et al. 1999), the European Alps (Campani et al., 2012), the Menderes Massif in Turkey (Hetzel et al., 2013), and western North America (e.g., Poage and Chamberlain, 2002; Horton et al., 2004; Takeuchi and Larson, 2005; Sjostrom et al., 2006; Mulch et al., 2008; Mix et al., 2011; Chamberlain et al., 2012). In addition, elevation histories of large mountain ranges provide climate model boundary conditions (e.g., Sewall et al., 2000; Bice and Marotzke, 2001; Herold et al., 2014; Rugenstein et al., 2014) that are used to simulate periods of warm temperatures and high CO_2 such as the early Eocene (e.g., Huber and Caballero, 2003, 2011; Lunt et al., 2012; Feng et al., 2013). Despite the importance of obtaining well-constrained topographic and climatic histories, and systematic advances in the field, there remains significant disagreement in well-studied mountain ranges such as the Sierra Nevada of California.

Debate surrounding the topographic evolution of the Sierra Nevada has centered on two primary hypotheses. First, mid- to late Cenozoic uplift is supported by westward-tilting sediments in paleochannels on the westward flanks of the Sierra Nevada (Unruh, 1991) and studies of fluvial incision and incision rates (e.g., Wakabayashi and Sawyer, 2001; Stock et al., 2004), although more recent cosmogenic isotope work indicates high paleorelief in the Pliocene (Stock et al., 2005). Uplift and increased incision since the Pliocene are consistent with tectonic models calling for the removal of dense (e.g., eclogitic) lower lithosphere beneath the southern Sierra (Ducea and Saleeby, 1998; Saleeby et al., 2003; Zandt et al., 2004; Levandowski et al., 2013). Seismic tomography indicates the presence of thick, high-velocity material beneath the southwestern foothills of the Sierra that dips to the east, suggesting that dense lithosphere has detached in the southern Sierra, whereas it has remained intact in the northern Sierra (e.g., Frassetto et al., 2011; Gilbert et al., 2012). Second, sedimentological (Cassel and Graham, 2011; Ingersoll, 2012), thermochronological (House et al., 1998), geomorphological

†hmix@scu.edu

 doi: 10.1130/B31294.1; 4 figures; 2 tables; Data Repository item 2015325.

Geological Society of America Bulletin, published online on 21 October 2015 as doi:10.1130/B31294.1

(Pelletier, 2007; Gabet, 2014), and stable isotope studies have indicated paleoelevations similar to modern elevations as early as the middle Miocene (Mulch et al., 2008) or even the Oligocene or Eocene (Mulch et al., 2006; Cassel et al., 2009; Hren et al., 2010). Geologic mapping indicates erosion along the Sierra Nevada batholith axis, suggesting the late Mesozoic Sierra formed a paleodivide prior to the deposition of Eocene fluvial sediments (Van Buer et al., 2009). Furthermore, seismic, thermobarometric, and magnetotelluric studies are at odds with rapid uplift in the late Cenozoic (e.g., Wernicke et al., 1996). These studies suggest Sierran surface uplift during the Late Cretaceous or early Cenozoic, possibly representing the edge of a large continental plateau (e.g., Garside et al., 2005; Cassel et al., 2012, 2014) and subsequent minor changes in relief and elevation during the Cenozoic (e.g., House et al., 1998; Cecil et al., 2006; Crowley et al., 2008; Mulch et al., 2008).

Stable isotope paleoaltimetry exploits the systematic depletion of deuterium and ^{18}O of atmospheric moisture during orographic rainout (cf. Chamberlain and Poage, 2000; Garzione et al., 2000; Rowley et al., 2001; Blisniuk and Stern, 2005; Rowley and Garzione, 2007). In the case of the western Sierra Nevada, Pacific Ocean–derived air masses advect eastward and become progressively depleted in moisture as they rise eastward over the Sierran crest. As such, the dominant control on $\delta^{18}O$ and δD of modern precipitation ($\delta^{18}O_{precip}$ and δD_{precip} hereafter) in the western Sierra Nevada is elevation (Friedman and Smith, 1970; Smith et al., 1979; Ingraham and Taylor, 1991; Friedman et al., 1992).

So far, geochemical studies in the western Sierra Nevada have relied on hydrogen isotopes in authigenic kaolinite (Mulch et al., 2006), hydrated volcanic glass (Mulch et al., 2008; Cassel et al., 2009), and long-chain *n*-alkanes as well as soil tetraether geochemistry (Hren et al., 2010). While these studies have offered insight into Sierran paleoelevation, some recent work has called into question the ability of materials such as kaolinite to preserve meteoric water signals without undergoing hydrogen isotope exchange (Wakabayashi, 2013).

Previous work in weathering environments has demonstrated that halloysite and other clay minerals such as allophane or imogolite may act as metastable precursors to kaolinite (O'Neil and Kharaka, 1976; Steefel and Van Cappellen, 1990; Jeong, 1998; Joussein et al., 2005). Hydrogen has been shown to exchange with the hydrated halloysite-10Å but not the dehydrated halloysite-7Å or kaolinite (Savin and Hsieh, 1998; Hsieh and Yapp, 1999; Joussein et al., 2005; Renac and Assassi, 2009). The time to δD "isotopic closure" is unknown and likely varies with climate, soil pCO_2, and water availability (Sieffermann and Millot, 1969; Ziegler et al., 2003). Similar to hydrogen, oxygen is incorporated from meteoric water during weathering from feldspars to clay minerals. However, no measurable oxygen isotope exchange has been observed for halloysite (7Å and 10Å) or kaolinite (Lawrence and Taylor, 1971; O'Neil and Kharaka, 1976; Sheppard and Gilg, 1996; Ziegler et al., 2003) under Earth surface conditions. Moreover, while kaolinite has been observed to undergo hydrogen isotope exchange at temperatures as low as 40 °C, the oxygen isotope ratios of kaolinite appear to be much more resistant to diagenetic alteration (Longstaffe and Ayalon, 1990).

Thus, to investigate potential hydrogen isotope exchange, we measured the oxygen isotope composition of kaolinite within well-described Eocene auriferous gravels (e.g., Mulch et al., 2006; Cassel and Graham, 2011; Fig. 1). These samples are the same as those measured in the hydrogen isotope study of Mulch et al. (2006). These oxygen isotope data confirm the results of existing stable isotope studies in two ways. First, an east-west oxygen isotope gradient confirms initial hydrogen isotope studies, and associated paleoelevation estimates are in line with existing estimates from multiple proxy materials. Second, paleothermometry indicates that these kaolinites reflect near-surface conditions. Our findings add to the robustness of existing constraints supporting high topography and a warm climate in the Sierra Nevada during the early Eocene.

METHODS

Kaolinite Sampling, Preparation, and Isotopic Analysis

We analyzed the oxygen isotope ratios of 16 kaolinite samples from 13 localities along the Eocene American and Yuba Rivers in the northern Sierra Nevada (Fig. 1). The auriferous gravels contain fossil floral assemblages that range from early to latest Eocene and are overlain by volcaniclastic strata radiometri-

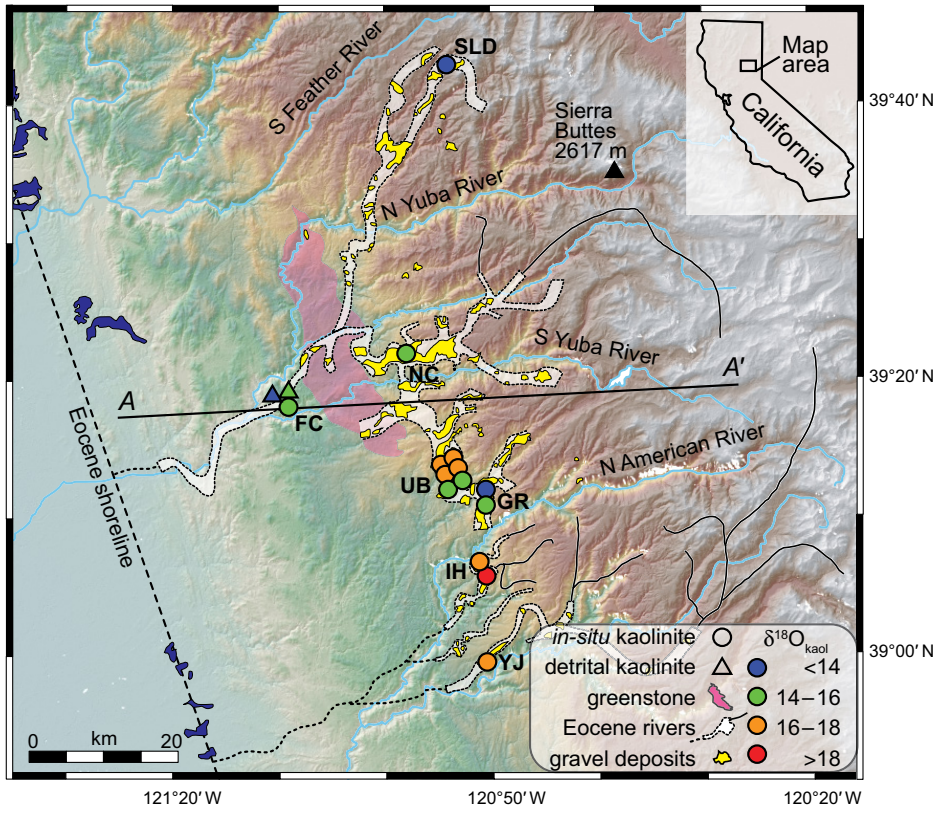

Figure 1. Map of early Eocene fluvial networks (white), gravel deposits (yellow), and mean kaolinite $\delta^{18}O$ values (circles, ‰) from the ancestral Yuba and American Rivers used in this study (Table 1). Transect A-A′ denotes the profile used in Figure 2. Shaded region is greenstone, interpreted as Paleogene ridge in Figure 3C. SLD—Saint Louis, FC—French Corral, NC—North Columbia, UB—You Bet, GR—Gold Run, IH—Iowa Hills, YJ—Yankee Jim's Mine.

Geological Society of America Bulletin, published online on 21 October 2015 as doi:10.1130/B31294.1

cally dated as old as early Oligocene, 31.2 Ma (summarized in Cassel et al., 2012). Typically, labile granite clasts in the auriferous gravels are altered to kaolinite, and the unaltered character of the overlying volcaniclastic sequence demonstrates that kaolinitic weathering occurred during the Eocene. We distinguish between in situ kaolinites that formed by weathering of granitic pebbles in the gravel deposits and detrital kaolinites. In situ kaolinite samples were separated from the individual granite clasts. Detrital kaolinite samples were obtained from Yuba River channel sand deposits that were transported downstream as part of the Eocene river system. All kaolinite samples analyzed in this study are from Mulch et al. (2006). Kaolinite samples were centrifuged to the 1–2 µm size fraction, dried, and subsequently mixed with LiF and pressed into pellets to prevent dispersion during lasing. Samples were isolated in a Fisher Scientific Isotemp vacuum oven at 80 °C and –100 kPa for at least 3 d before isotopic analysis. Oxygen isotope composition was determined using a Thermo Finnigan MAT 252 mass spectrometer and a laser fluorination line (e.g., Sharp, 1990; Sjostrom et al., 2006; Mix and Chamberlain, 2014). Samples were exposed to three 90 s preflourinations with BrF_5 in order to liberate impurities from the samples and fluorination line. The O_2 gas was liberated from the samples by reaction with BrF_5 using a New Wave Research MIR10-25 infrared laser ablation system. Oxygen gas was purified through two liquid nitrogen cold traps and a KBr trap before being introduced to the mass spectrometer. Analyses were controlled with repeated analyses of NBS-28 quartz, which demonstrated the precision of this method to be <0.2‰. All isotopic ratios are reported with respect to Vienna standard mean ocean water (VSMOW). Depending on the quantity of sample, duplicate or triplicate kaolinite oxygen isotope ($\delta^{18}O_{kaol}$) measurements were made.

Midlatitude Eocene Sea-Level $\delta^{18}O$ and δD Constraints

Stable isotope constraints from coastal regions are essential for paleoenvironmental reconstructions. Not only do paleoaltimetry models rely on the input of sea-level constraints (e.g., Rowley et al., 2001), but recent work has demonstrated the necessity of determining the isotopic continentality effect in order to deconvolve the roles of changing moisture source, vapor recycling, and orographic rainout (e.g., Mix et al., 2013; Chamberlain et al., 2014; Winnick et al., 2014). Mulch et al. (2006) produced the first Eocene sea-level δD_{precip} (–43‰) estimate using a linear regression of kaolinite hydrogen isotope composition and distance from the Eocene shoreline. In order to allow the most direct comparison between oxygen and hydrogen isotope compositions, we determined the sea-level $\delta^{18}O_{kaol}$ value to be 18.3‰ ± 0.6‰ (sea-level $\delta^{18}O_{precip}$ = –7.1‰) using the sea-level δD_{kaol} value of –80‰ ± 5‰ (Mulch et al., 2006), the global meteoric water relationship ($\delta D = 8 \times \delta^{18}O + 10$; Craig, 1961), and the kaolinite-water equilibrium fractionation factors for oxygen and hydrogen (Sheppard and Gilg, 1996) at 20 °C. These constraints are in line with independent estimates of Eocene temperature (e.g., Wolfe, 1994; Chase et al., 1998; Wolfe et al., 1998; Yapp, 2008; Hren et al., 2010) and modern meteoric water relationships in the Sierra Nevada (e.g., Oster et al., 2012). These kaolinite-based sea-level values are nearly identical to those derived from the hydrogen isotope composition of leaf *n*-alkanes (Hren et al., 2010), but they are somewhat less depleted in ^{18}O and D than those measured in an Eocene coastal Oxisol (δD_{precip} = –61‰, $\delta^{18}O_{precip}$ = –8.9‰; Yapp, 2008). Cassel et al. (2009) determined the δD of hydrated volcanic glass from the coastal Ione Formation to be –105‰ (n = 2 samples). This constraint is not amenable to direct comparison with these kaolinite and goethite values because it represents the Eocene–Oligocene time interval as opposed to the warmer early Eocene, and glass-water fractionation is not temperature dependent (Friedman et al., 1993).

Calculating Paleoelevations

We used the thermodynamic model of Rowley et al. (2001), which utilizes the difference in mineral $\delta^{18}O$ values between a given study area and a sea-level value in order to infer the difference in precipitation-weighted hypsometric mean elevation between the two sites. The model simulated moisture source conditions off the west coast of North America in the Eocene Pacific Ocean along with the equilibrium isotopic fractionation between water vapor and condensation during rainout. We used a sea-level $\delta^{18}O_{kaol}$ value of 18.3‰ ± 0.6‰ using the same approach as Mulch et al. (2006) (see previous description). Our error estimates account for two sources of uncertainty in calculated Eocene paleoelevations. First, paleoaltimetry errors due to uncertainty in the isotopic lapse rate were determined by randomly sampling 1000 pairs of simulated Eocene humidity and temperature between 31.5°N and 46.4°N and 123.8°W and 146.3°W (Huber and Caballero, 2003). Second, the uncertainty estimates also incorporate uncertainty in the sea-level estimate of ±0.6‰ in $\delta^{18}O$ values (±5‰ in δD; Mulch et al., 2006).

Assessing Paleotemperatures

We exploited differences in the hydrogen and oxygen equilibrium isotope fractionation in order to calculate the temperature of kaolinite formation. The kaolinite-water oxygen isotope fractionation factor ($1000\ln\alpha_{kaol\text{-}water} = 2.76 \times 10^6 T^{-2} - 6.75$) is positive, meaning that at equilibrium, the mineral is enriched in ^{18}O relative to the water present during mineral growth (Sheppard and Gilg, 1996). In contrast, the hydrogen isotope fractionation factor is negative ($1000\ln\alpha_{kaol\text{-}water} = -2.2 \times 10^6 T^{-2} - 7.7$; Sheppard and Gilg, 1996). Assuming that the minerals formed in equilibrium with surface water and shallow groundwaters of meteoric origin, these fractionation factors of opposing slopes can be combined with the global meteoric water relationship to calculate temperatures:

$$3.0350 \times 10^6 T^{-2} = \delta^{18}O_{kaol} - 0.1250\delta D_{kaol} + 7.0375, \quad (1)$$

where T is absolute temperature. This approach has been used in paleoclimatic, diagenetic, and other geothermometry applications with kaolinite and other phyllosilicates (e.g., Savin and Epstein, 1970; Delgado and Reyes, 1996; Vitali et al., 2002; Tabor and Montañez, 2005; Gilg et al., 2013; Mix and Chamberlain, 2014).

Temperatures were calculated for all samples with paired $\delta^{18}O_{kaol}$ and δD_{kaol} measurements (Table DR1[1]). We did so by calculating temperatures for all possible measurement pairs (n = 2–6 pairs for all 16 samples) of a given sample using Equation 1. The $\delta^{18}O_{kaol}$ and δD_{kaol} measurement errors for each individual pair were combined by propagating at 1σ as the square root of the sum of the variances.

The reported temperatures and errors for each sample were calculated using an error-weighted mean with errors propagated using a Student's t multiplier (e.g., Ma et al., 2005; Berger et al., 2006; Maher et al., 2007; Halevy et al., 2011; Ibarra et al., 2014). Typically, due to higher associated error with the precision of the $\delta^{18}O_{kaol}$ measurement (±0.3‰–1.6‰), compared to the δD_{kaol} measurements (±2‰), temperature errors are dominated by the $\delta^{18}O_{kaol}$ error (as high as 4.5 °C). By using an error-weighted average, we accounted for the variable error associated with the $\delta^{18}O_{kaol}$ measurement on duplicate measurements of a single sample (see Table DR1 [see footnote 1]). To emphasize the conservative nature of the error propagation scheme, we

[1]GSA Data Repository item 2015325, Table DR1, containing δD-$\delta^{18}O$ sample pairs and temperature calculations, is available at http://www.geosociety.org/pubs/ft2015.htm or by request to editing@geosociety.org.

also report the mean square weighted deviation (MSWD), where the MSWD is the ratio of the observed scatter to the scatter expected from the analytical error.

RESULTS

Oxygen Isotope Geochemistry and Paleoaltimetry

The oxygen isotope composition of in situ kaolinite decreases systematically upstream (eastward). The $\delta^{18}O_{kaol}$ values of kaolinitized clasts range from 14.7‰ to 19.2‰ (n = 14) at 32–56 km east of the Eocene shoreline, while samples between 84 and 86 km inland range from 11.4‰ to 14.4‰ (Fig. 2B). These $\delta^{18}O_{kaol}$ values translate to Eocene paleoelevations that increase systematically upward to 2400 m at the easternmost localities (Table 1; Fig. 2C). We analyzed two detrital kaolinites separated from channel sands 32 km east of the Eocene shoreline. These samples have lower $\delta^{18}O$ values of 13.3‰ and 15.7‰, both of which are more depleted in ^{18}O than in situ kaolinites from the same location (Table 1; Fig. 2B). These $\delta^{18}O$ values likely reflect higher-elevation conditions as compared to the detrital kaolinites and were transported from upstream following kaolinitization by the Eocene river system, as previously suggested by Mulch et al. (2006).

Kaolinite Paleothermometry

Weathering temperatures calculated based on multiple δD (n = 31) and $\delta^{18}O$ (n = 32) analyses from the 16 kaolinite samples (14 kaolinitized clasts, 2 detrital samples) ranged from 13.0 °C to 36.7 °C (Table 1; Fig. 3B). MSWD values from individual samples ranged from 10^{-30} to 20.49 and exhibited no correlation with the number of $\delta^{18}O$-δD pairs used to calculate temperatures for each sample. A MSWD <1, exhibited for 10 of 16 samples with temperature estimates, implies an overestimation of analytical errors. Six samples exhibited MSWD >1, typically driven by discrepancies in the duplicate or triplicate $\delta^{18}O_{kaol}$ measurements (Table DR1 [see footnote 1]). The mean of these samples gives an estimated temperature in the Eocene Sierra Nevada of 23.2 ± 6.4 (1σ) °C.

DISCUSSION

Quantitative constraints on paleoelevation and climate are essential in unlocking the tectonic history of western North America. Here, we discuss our results in the context of modern meteoric water isotope systematics and existing paleoclimate records from the Cenozoic Sierra Nevada.

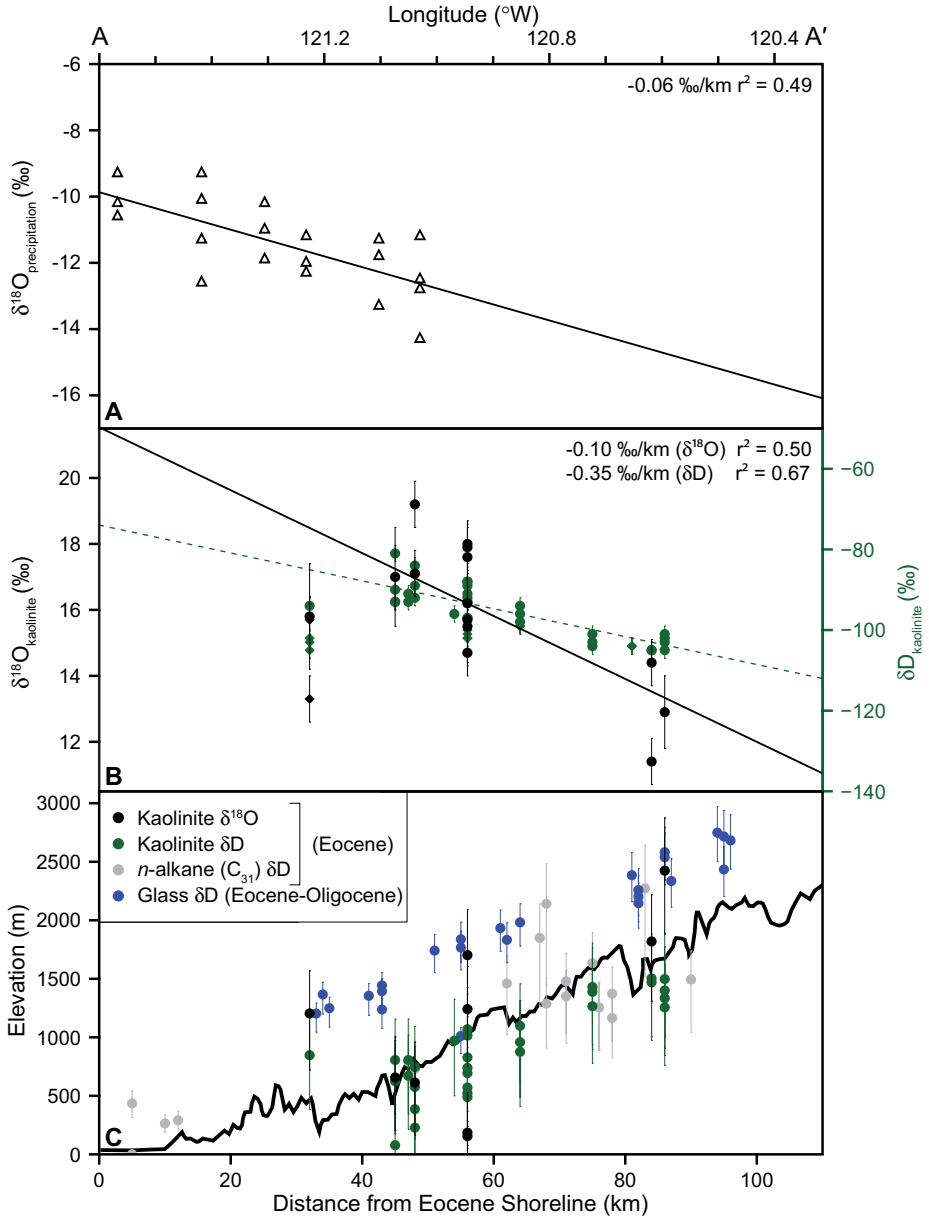

Figure 2. (A) Modern $\delta^{18}O_{precip}$ collected during winter 1984–1985 (Ingraham and Taylor, 1991). (B) Kaolinite $\delta^{18}O$ (black) and δD (green) vs. distance to the Eocene shoreline. In situ samples are circles; detrital samples are diamonds. Linear regressions of $\delta^{18}O$ and δD are through all in situ measurements from each sample set. (C) Reconstructed Eocene elevations from kaolinite $\delta^{18}O$ (this study), kaolinite δD (Mulch et al., 2006), n-alkane δD (Hren et al., 2010), and glass δD (Cassel et al., 2009).

Oxygen and Hydrogen Isotope Gradients and Variability in the Western Sierra Nevada

In order to assess differences in elevation and hydrologic regime between the modern and Paleogene Sierra Nevada, we compared stable isotope gradients from the Eocene coastline (the modern eastern Central Valley) to the range crest. The modern $\delta^{18}O$ precipitation gradient is –0.06‰ ± 0.01‰/km along the western flank of the Sierra (1σ; Fig. 2A; Ingraham and Taylor, 1991). Elevated continental isotope gradients of this nature are restricted to the windward flanks of mountain ranges, as isotope gradients over flatter regions are typically an order of magnitude lower (Rozanski et al., 1993; Winnick et al., 2014). Nonetheless, these gradients are lower than predicted by an open-system Rayleigh distillation model, indicating the important

TABLE 1. STABLE ISOTOPE MEASUREMENTS OF KAOLINITE FROM THE EOCENE, NORTHERN SIERRA NEVADA, CALIFORNIA

Sample	Sample coordinates	Distance to Eocene shore (km)	Modern elevation (m)	δD (‰, VSMOW)*	$\delta^{18}O$ (‰, VSMOW)	Eocene δD elevation*,† (m) (±)	Eocene $\delta^{18}O$ elevation† (m) (±)	Temperature§ (°C)	δD-$\delta^{18}O$ temperature pairs (no.)
Yuba River samples									
01-SLD05	(39.7000°N, 120.9185°W)	86	1556	–102 ± 2	12.9 ± 1.1	1334 (+370/–490)	2424 (+451/–535)	31.6 ± 2.1	2
02-SLD05	(39.7000°N, 120.9185°W)	86	1556	–105 ± 2	–	1498 (+379/–498)			
04-LP05w	(39.6884°N, 120.9845°W)	86	1524	–101 ± 2	–	1256 (+366/–496)			
04-LP05b	(39.6884°N, 120.9845°W)	86	1524	–103 ± 2	–	1400 (+373/–493)			
04-OF05	(39.4315°N, 120.8355°W)	75	1237	–103 ± 2	–	1389 (+373/–493)			
W-2-04	(39.3388°N, 120.8040°W)	75	1183	–104 ± 2	–	1430 (+375/–494)			
W-3-04	(39.3388°N, 120.8040°W)	75	1183	–101 ± 2	–	1266 (+367/–487)			
M-1-04	(39.3659°N, 120.9241°W)	64	927	–98 ± 2	–	1098 (+359/–478)			
M-3-04	(39.3659°N, 120.9241°W)	64	927	–94 ± 2	–	876 (+352/–466)			
M-4-04	(39.3659°N, 120.9241°W)	64	927	–96 ± 2	–	959 (+354/–471)			
03-NC05	(39.3631°N, 120.9935°W)	56	854	–92 ± 2	15.7 ± 1.4	739 (+348/–458)	1241 (+365/–486)	24.5 ± 2.1	2
02-CD05	(39.3676°N, 121.0338°W)	54	790	–96 ± 2	–	971 (+355/–471)			
FC-04_1	(39.3005°N, 121.1555°W)	32	472	–94 ± 2	15.8 ± 1.6	847 (+351/–464)	1204 (+364/–484)	22.8 ± 4.5	4
GR-3-04	(39.1773°N, 120.8548°W)	84	975	–105 ± 2	14.4 ± 0.7	1503 (+379/–498)	1819 (+400/–511)	23.6 ± 0.6	4
GR-5-04	(39.1773°N, 120.8548°W)	84	975	–105 ± 2	11.4 ± 0.7	1470 (+377/–496)	2949 (+506/–558)	36.7 ± 0.6	6
09-UB05	(39.2070°N, 120.8999°W)	56	914	–88 ± 2	16.2 ± 1.2	522 (+345/–444)	1028 (+357/–475)	25.2 ± 2.4	6
10-UB05	(39.2070°N, 120.8999°W)	56	914	–91 ± 2	15.5 ± 1.1	695 (+347/–455)	1351 (+371/–491)	26.9 ± 1.3	4
11-UB05	(39.2070°N, 120.8999°W)	56	914	–89 ± 2	17.6 ± 0.9	571 (+345/–448)	361 (+344/–433)	16.5 ± 0.8	6
02-UB05	(39.2122°N, 120.8864°W)	56	914	–97 ± 2	–	1069 (+358/–477)			
05-UB05	(39.2122°N, 120.8864°W)	56	914	–97 ± 2	18.0 ± 0.7	1015 (+356/–474)	155 (+344/–418)	13.0 ± 1.5	4
07-UB05	(39.2070°N, 120.8999°W)	56	914	–93 ± 2	14.7 ± 0.7	828 (+350/–463)	1702 (+391/–506)	28.3 ± 0.7	4
08-UB05	(39.2070°N, 120.8999°W)	56	914	–88 ± 2	17.9 ± 0.7	490 (+344/–442)	185 (+344/–421)	17.4 ± 1.0	2
American River samples									
01-IH05	(39.1032°N, 120.8628°W)	48	867	–92 ± 2	17.1 ± 0.7	746 (+348/–458)	614 (+346/–450)	18.8 ± 1.3	2
03-IH05	(39.1032°N, 120.8628°W)	48	867	–84 ± 2	19.2 ± 0.7	228 (+344/–426)	–478 (+360/–364)	14.7 ± 0.8	2
04-IH05	(39.1032°N, 120.8628°W)	48	867	–86 ± 2	–	386 (+344/–435)			
05-IH05	(39.1032°N, 120.8628°W)	48	867	–89 ± 2	–	576 (+345/–447)			
02-BD05a	(39.0920°N, 120.8475°W)	47	914	–93 ± 2	–	806 (+350/–462)			
02-BD05b	(39.0920°N, 120.8475°W)	47	914	–91 ± 2	–	671 (+347/–455)			
01-YJ05	(39.0312°N, 120.8628°W)	45	803	–90 ± 2	17.0 ± 1.5	625 (+346/–451)	657 (+347/–453)	22.7 ± 4.2	4
03-YJ05	(39.0312°N, 120.8628°W)	45	803	–81 ± 2	–	78 (+345/–411)			
04-YJ05	(39.0312°N, 120.8628°W)	45	803	–93 ± 2	–	806 (+350/–462)			
05-YJ05	(39.0312°N, 120.8628°W)	45	803	–93 ± 2	–	806 (+350/462)			
Yuba River detrital samples									
FC1-04	(39.3005°N, 121.1555°W)	32	472	–102 ± 2	15.7 ± 0.7			19.1 ± 0.7	4
FC4-04	(39.3005°N, 121.1555°W)	32	472	–103 ± 2	13.3 ± 0.7			29.1 ± 0.9	4

Note: VSMOW—Vienna standard mean ocean water.

*The δD measurements and elevations are from Mulch et al. (2006)

†Elevation uncertainty measurements (1σ) include both the lapse-rate determination and the sea-level isotope composition of precipitation.

§Temperatures and temperature uncertainty (1σ) were determined using an error-weighted average for all δD-$\delta^{18}O$ pairs from a given sample (2 to 6 pairs per sample; see Table DR1 [see text footnote 1]).

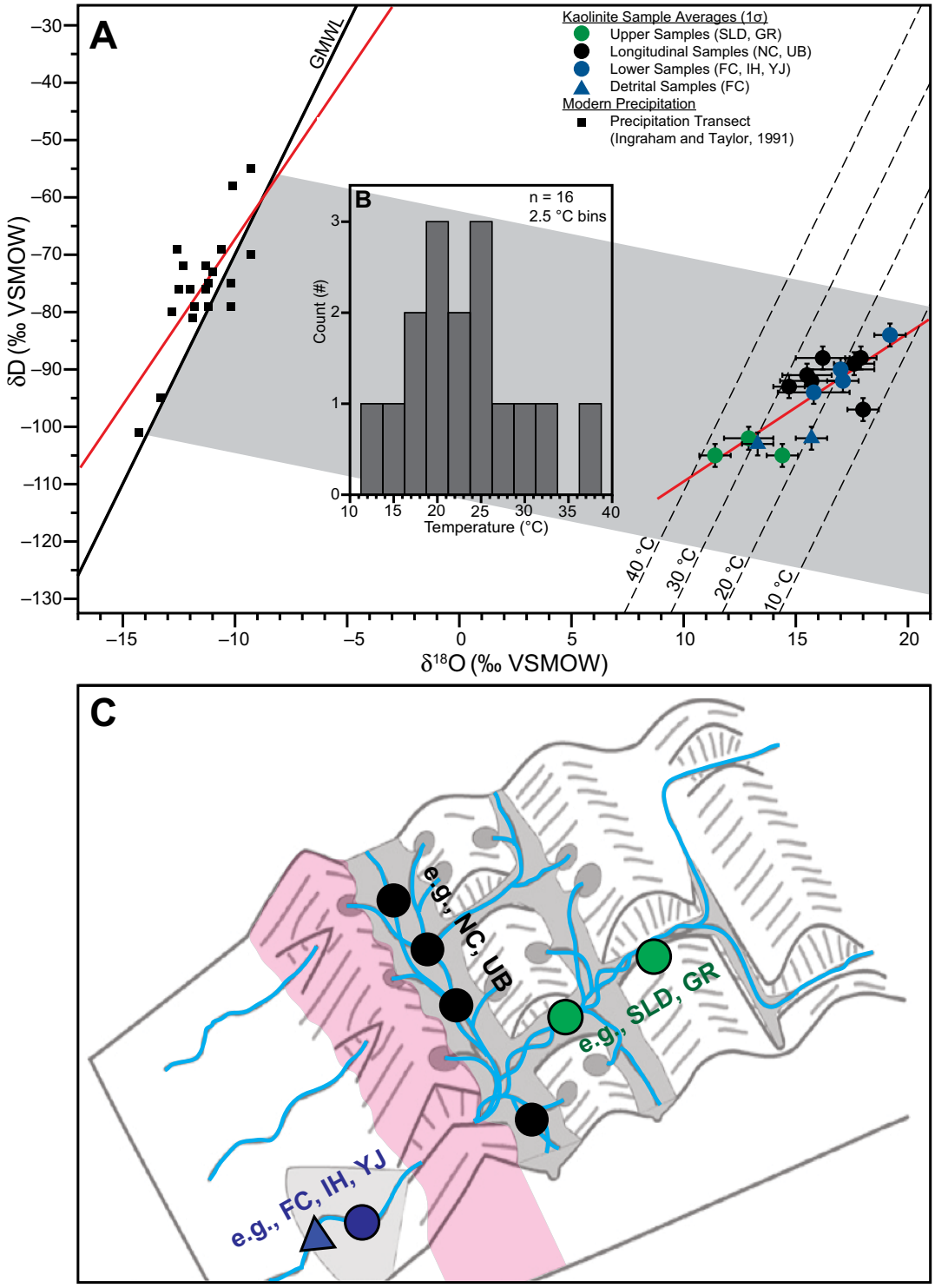

Figure 3. (A) $\delta^{18}O$-δD relationships in modern meteoric water and Eocene kaolinites. Dashed lines are kaolinite temperature lines parallel to global meteoric water line. Shaded region is 95% confidence interval from modern meteoric waters in the Sierra Nevada. (B) Histogram of kaolinite mineral formation temperatures. (C) Reconstructed depositional environments of in situ kaolinites. Localities are grouped into upper transverse (green), longitudinal (black), and lower transverse (blue) segments of the Paleogene Yuba and American Rivers. Shaded region represents greenstone ridge of Figure 1. Figure is after Cassel and Graham (2011) and Gabet (2014). VSMOW—Vienna standard mean ocean water; GMWL—global meteoric water line. SLD—Saint Louis, FC—French Corral, NC—North Columbia, UB—You Bet, GR—Gold Run, IH—Iowa Hills, YJ—Yankee Jim's Mine.

Geological Society of America Bulletin, published online on 21 October 2015 as doi:10.1130/B31294.1

role of evapotranspiration in recycling moisture (~20%) in northern and central California (Ingraham and Taylor, 1991).

Most stable isotope paleoaltimetry studies have focused on the western flank of the northern Sierra Nevada because multiple proxies are available in well-studied and well-preserved Eocene fluvial sediments. Previous isotope studies from these Eocene sediments utilized three different proxy materials: kaolinite, hydrated volcanic glass, and leaf wax *n*-alkanes. These three records all exhibit the same eastward depletion of D, though the degree of this depletion varies. Mulch et al. (2006) documented a decrease of 25‰ in δD between the westernmost and easternmost sites. With a reconstructed Eocene sea-level δD_{kaol} value of 76‰ derived from linear regression, this translates to ~30‰ between the Eocene shoreline (Ione Formation) and sites 80–100 km inland. The fossil angiosperm *n*-alkane record of Hren et al. (2010) exhibited a similar 30‰ decrease in δD values, while hydrated volcanic glass indicated the greatest isotopic gradient (ΔδD = ~48‰; Cassel et al., 2009). The kaolinite $\delta^{18}O$ record presented here shows a decrease of ~5‰ between the westernmost and easternmost localities, in agreement with prior paleoaltimetry studies. Furthermore, Eocene kaolinite isotope gradients (–0.10‰ ± 0.03‰/km in $\delta^{18}O$) are similar to the modern isotope gradient (–0.06‰ ± 0.01‰/km; Fig. 2B; Ingraham and Taylor, 1991).

Subsequent studies have noted the persistence of an isotope gradient across the Sierra Nevada through Neogene time. Crowley et al. (2008) interpreted a decrease in $\delta^{18}O$ in mammalian tooth enamel between the windward and leeward sides of the Sierra as evidence of a rain shadow dating to at least 16 Ma. Similarly, hydrated volcanic glass from the Coast Ranges, Sierra Nevada, and Basin and Range exhibit isotopic evidence for a rain shadow since the middle Miocene (Mulch et al., 2008). Isotopic studies of pedogenic carbonate and smectite (e.g., Poage and Chamberlain, 2002; Horton and Chamberlain, 2006) documented low-$\delta^{18}O$ moisture in the Neogene Basin and Range, with increasing $\delta^{18}O$ values since the middle Miocene. Originally thought to be due to the topographic lowering of the Basin and Range Province and increased influence of high-$\delta^{18}O$ moisture associated with the North American Monsoon (e.g., Horton and Chamberlain, 2006), these Miocene to Pleistocene isotope records have since been interpreted as evidence of the increased role of continental vapor recycling since the middle Miocene (Mix et al., 2013; Chamberlain et al., 2014).

Relationships between oxygen and hydrogen isotopes in meteoric water can illuminate far more about the regional hydrologic cycle than is possible with a single-isotope system. Globally, oxygen and hydrogen isotopes vary sympathetically along a well-established meteoric water line ($\delta D = 8 \times \delta^{18}O + 10$; Craig, 1961). Multiyear monitoring of precipitation in the western Sierra Nevada at an elevation of 676 m falls on a local meteoric water line of $\delta D = 7.9 \times \delta^{18}O + 9.3$ ($n = 31$, $r^2 = 0.98$; Oster et al., 2012). However, due to kinetic effects associated with postcondensation evaporation and vapor recycling, $\delta^{18}O$-δD lines along spatial transects may deviate significantly from global and even local meteoric water relationships (e.g., Gat and Matsui, 1991). For example, the only existing modern transect of precipitation in our study region was collected during the 1984–1985 winter by Ingraham and Taylor (1991) (Fig. 2A), and it produces a water line of $5.9 \times \delta^{18}O + 14.5$ ($n = 20$, $r^2 = 0.56$; Fig. 3A). A longer transect from the modern coast into the Great Basin indicates a variety of local hydrologic regimes relating primarily to differences in water balance. Such transitions from open (i.e., windward flanks of mountain ranges where rainout dwarfs evapotranspiration) to closed (i.e., vapor recycling equal to or greater than precipitation) systems can produce great differences in local meteoric water line characteristics (Ingraham and Taylor, 1991; Winnick et al., 2014).

The $\delta^{18}O$-δD characteristics of surface waters along a transect may differ from local meteoric water relationships for a variety of reasons. Evaporation both enriches residual soil or surface water in ^{18}O and D as well as decreases the slope of the $\delta^{18}O$-δD line due to differences in kinetic fractionation. For example, modern evaporation lines from surface waters in the Sacramento Valley, Warner Range, and Truckee River suggest $\delta^{18}O$-δD slopes of 5.3–6.6 (Ingraham and Taylor, 1989; Horita, 1990; Benson and White, 1994). Recycling of this evaporatively enriched water along a transect could serve to decrease the $\delta^{18}O$-δD slope downwind, as observed in the modern Great Basin (Ingraham and Taylor, 1991).

While kaolinite does preserve the oxygen and hydrogen isotope ratios of parent water, in practice paleoclimate records may not reflect changes in meteoric water composition alone (e.g., Tabor and Montañez, 2005; Mix and Chamberlain, 2014; Oerter et al., 2014). Kaolinites from the Eocene Sierra Nevada plot on a $\delta^{18}O$-δD line with a slope of 2.4 ± 0.3 (1σ; Fig. 3A). This slope is significantly lower than that of modern precipitation (5.9 ± 1.3, 1σ) in the study region (Ingraham and Taylor, 1991). First, slopes lower than ~4 are too low to be explained by local evaporation only; however, such slopes can be produced through the recycling of evaporitic waters as discussed already. Second, $\delta^{18}O$-δD relationships in paleoclimate proxies can be affected by numerous factors, such as seasonal biases of mineral formation (e.g., Stern et al., 1997) and regional differences in weathering temperature (e.g., Mix and Chamberlain, 2014). Finally, the in situ clasts studied here were preserved adjacent to channelized sediments. As the weathering of granites occurred in overbank settings, kaolinites likely formed in equilibrium with evaporatively enriched waters (Figs. 3A and 3C). This would serve to both lower the slope of the $\delta^{18}O$-δD line, as observed and discussed already, and decrease oxygen isotope–based paleoelevation estimates (see following). Thus, we interpret the combined oxygen and hydrogen isotope geochemistry of Sierran kaolinites to be indicative of vapor recycling along the windward flank of the Sierra and preservation of evaporitic water signatures.

High-Elevation, High-Relief Eocene Northern Sierra Nevada

Given the reproducibility of this isotope gradient in multiple proxy materials and now in both the hydrogen and oxygen isotope systems, we interpret the systematic depletion of D and ^{18}O to be the result of orographic precipitation in the Eocene Sierra Nevada for a number of reasons. First, each of these materials has been shown to preserve isotopic compositions in both experimental and field settings. Furthermore, both the kaolinitized granite clasts examined here (Mulch et al., 2006) and the leaf fossils in these sediments (e.g., Wolfe, 1994; Chase et al., 1998; Wolfe et al., 1998; Hren et al., 2010) exhibit excellent preservation and lack physical evidence of deep burial diagenesis or isotopic exchange. Last, these records are consistent with the modern ~50‰ δD gradient of precipitation between the west and east sides of the range (Ingraham and Taylor, 1991). Back-trajectory analysis of modern air parcels in the Yuba River region indicate that air masses directly encounter Sierran topography, as opposed to complex moisture trajectories that wrap around other parts of the range (Oster et al., 2012; Lechler and Galewsky, 2013). The relatively simple modern orographic effect in this subregion of the Sierra further substantiates the argument that distillation of Pacific-derived moisture has been a dominant feature of the hydrologic regime since the Paleogene.

Here, we examine estimates of Sierran paleoelevation, relief, and morphology in light of these new stable isotope constraints. Mulch et al. (2006) observed elevations up to 1500 m in early Eocene ancestral Yuba River sediments and estimated the paleoelevations of the Sierra in excess of 2200 m. Similarly, Eocene leaf wax *n*-alkanes indicate paleoelevations >2200 m,

Geological Society of America Bulletin, published online on 21 October 2015 as doi:10.1130/B31294.1

while temperature lapse-rate estimates from glycerol dialkyl glycerol tetraethers (GDGTs) can exceed 3000 m and exhibit a greater range of reconstructed elevations (Hren et al., 2010). Oligocene hydrated volcanic glass produced the greatest paleoelevation estimates (~3200 m; Cassel et al., 2009; 2014). Our oxygen isotope–based reconstructions yield paleoelevations up to 2400 m, in agreement with hydrogen isotope–based estimates (Fig. 2C). Each of these studies has exploited the difference between the isotopic composition of materials from inland and coastal sites and a Rayleigh distillation model to estimate paleoelevation. As discussed earlier herein, this method models the orographic rainout of an air mass as it encounters topography in one dimension (Rowley et al., 2001). While this approach may not be adequately sophisticated for sites in the eastern Sierra Nevada and Basin and Range that receive moisture delivered via more complex trajectories (e.g., Galewsky, 2009; Lechler and Galewsky, 2013), the Yuba River region is ideal for simplified paleoaltimetry models. Similarly, complexities in atmospheric dynamics make it challenging to assess changes in orographic precipitation during the past (e.g., Molnar, 2010). For example, due to changes in atmospheric temperature lapse rates, stable isotope–based paleoelevations using global isotopic lapse rates can underestimate true relief by >14% and >40% at 2× and 4× preindustrial pCO_2, respectively (Poulsen and Jeffery, 2011). Nonetheless, given the proximity to the Pacific, prevailing westerly moisture transport in the midlatitudes of Cenozoic western North America, and Pacific-derived air parcel trajectories in the modern regime, we are confident that one-dimensional Rayleigh distillation models adequately represent westerly moisture transport in the Paleogene northern Sierra Nevada. Given that both elevated Eocene pCO_2 and evaporative effects serve to enrich kaolinites in ^{18}O, the paleoelevations presented here likely underestimate Eocene elevation.

While stable isotope paleoaltimetry confirms the existence of an elevation gradient similar to the modern gradient as early as the Eocene, these constraints are compatible with a wide range of scenarios for the tectonic evolution of the Sierra Nevada. It is increasingly clear that the topographic histories of the northern and southern Sierra Nevada differ substantially (e.g., Ducea and Saleeby, 1998; Saleeby et al., 2003; Zandt et al., 2004; Frassetto et al., 2011; Lechler and Niemi, 2011; McPhillips and Brandon, 2012; Gilbert et al., 2012; Levandowski et al., 2013). The stable isotope constraints presented in this work are restricted to the northern Sierra Nevada and cannot inform about the timing of surface uplift in the southern Sierra Nevada.

Geomorphic observations and subsequent modeling (e.g., Clark et al., 2005; Pelletier, 2007) support the existence of a high-elevation, low-relief relict landscape in the northern Sierra. Recent work revisiting geomorphic evidence suggests that paleovalleys in the northern Sierra Nevada were deeply incised by the Eocene, while observations in the southern Sierra are consistent with late Cenozoic uplift and incision (Gabet, 2014). Sedimentological work on the braided river deposits filling paleovalleys supports a steep-gradient, high-energy flow (e.g., Cassel and Graham, 2011) and the development of a trellised drainage network (e.g., DeGraaff-Surpless et al., 2002; Gabet, 2014) during the early Cenozoic. While stable isotope constraints, which represent the precipitation-weighted hypsometric mean elevation of a catchment (e.g., Rowley et al., 2001), can neither confirm nor deny the amount of relief in Paleogene incised valleys, it is interesting to note the compatibility of these new findings with a trellised drainage network. Notably, samples from French Corral, located ~30 km east of the Eocene shoreline and to the west of a bedrock ridge, have lower $\delta^{18}O$ and δD (and thus higher calculated paleoelevations) than expected by the trend line of samples farther to the east. Though there are insufficient data to examine the robustness of this finding, we speculate that these higher paleoelevations from the French Corral locality may represent runoff from the high coastal ridgeline suggested by geological and geomorphic observations (Figs. 1 and 3C). In summation, we argue that the stable isotope–based paleoelevation record presented here is consistent not only with prior isotopic studies, but also with observations from a variety of fields. This work demonstrates that geomorphic, sedimentologic, thermochronologic, and stable isotope studies have become increasingly compatible in their support for a northern Sierra Nevada that stood high during the Paleogene. Late Cenozoic uplift and incision occurring as a result of crustal delamination were certainly limited in their contribution to modern Sierran elevation, particularly in the northern part of the range.

Kaolinite-Based Paleothermometry in the Context of Existing Constraints

Combined $\delta^{18}O$- and δD-based kaolinite temperatures confirm the preservation of near-surface water compositions and weathering environments. Kaolinite weathering temperatures range from 13.0 °C to 36.7 °C, with a mean of 23.2 ± 6.4 °C (1σ, $n = 16$) for the Eocene northern Sierra Nevada (Tables 1 and 2; Table DR1 [see footnote 1]). For all but two kaolinite samples, the temperatures are at least 10 °C cooler than diagenetic temperatures at which hydrogen isotopes have been observed to begin isotopic exchange, and even further from undergoing oxygen isotope exchange (Longstaffe and Ayalon, 1990). This constraint supports field observations that kaolinite samples reflect weathering in situ and the conditions of the surface environment, further substantiating their appropriateness for paleoenvironmental reconstructions.

While this technique is sufficient for producing a single temperature estimate of the Eocene Sierra Nevada, several issues preclude the cal-

TABLE 2. COMPILATION OF EOCENE TEMPERATURE ESTIMATES OF THE SIERRA NEVADA REGION

Material/method	Age	Latitude (°N)	Longitude (°W)	Temperature* (°C)	Reference
Observations					
Kaolinite	Early Eocene	39.3	120.9	23.2 ± 6.4	This study
Biomarker	Early Eocene	39.3	121.0	16.6 ± 4.7	Hren et al. (2010)
Paleofloral	Late Eocene	39.7	120.0	22.3 ± 1.0	Chase et al. (1998)
Paleofloral	Late Eocene	39.7	120.0	23.0 ± 1.3	Wolfe et al. (1998)
Goethite	Early Eocene	38.3	120.9	21.0 ± 4.0	Yapp (2008)
Paleofloral	Middle Eocene	39.2	121.1	16.5 ± 1.0	Wolfe (1994)
Paleofloral	Early Eocene	39.1	120.9	15.3 ± 3.2	Hren et al. (2010)
Paleofloral	Early Eocene	39.2	120.9	15.2 ± 2.7	Hren et al. (2010)
Paleofloral	Early Eocene	39.2	120.9	16.3 ± 2.5	Hren et al. (2010)
Models					
CCSM1.4	Early Eocene, 2240 ppm	~40	~120	23.7	Huber and Caballero (2011)
CCSM1.4	Early Eocene, 4480 ppm	~40	~120	27.2	Huber and Caballero (2011)

*Temperature errors are all 1σ.

culation of Eocene altitudinal or temperature gradients. First, individual sample temperatures are too scattered to produce a statistically robust gradient. Second, uncertainty in the kaolinite-water fractionation at low temperatures (see Sheppard and Gilg, 1996) is likely greater than the resolution necessary for temperature-based paleoaltimetry reconstructions, at least across this modest climatic gradient. Finally, gradients in temperature and elevation vary greatly in the modern regime, both spatially and seasonally. For example, altitudinal lapse rates in 39 regions with surface topography >750 m range from 3.6 to 8.1 °C/km on an annual basis (Meyer, 1992), and lapse rates in the modern Cascades are as low as 2.5 °C/km during the summer (Minder et al., 2010). Furthermore, coast to interior temperature gradients along the windward flanks of mountain ranges can differ substantially from lapse rates in those regions. Summer maximum temperatures actually increase from the coast to the interior in northern California's Klamath Mountains (Johnstone and Dawson, 2010).

Temperature records from the Eocene Sierra Nevada are critical to unlocking regional climate heterogeneity in western North America and characterizing temperatures at a range of elevations during a time of high atmospheric pCO_2. Kaolinite weathering temperatures are in agreement with these existing observations and models of the Eocene Sierra Nevada (Fig. 4). Yapp (2008) used the oxygen and hydrogen isotope geochemistry of a coastal Oxisol to determine an estimate of 21 ± 4 °C. These geochemical reconstructions from in situ kaolinite and pedogenic goethite are higher than the 16.6 ± 4.7 °C estimate from leaf *n*-alkanes (Hren et al., 2010) and early Eocene leaf physiognomy studies (Wolfe, 1994; Hren et al., 2010). Somewhat surprisingly, leaf physiognomy estimates from the globally cooler late Eocene (Chase et al., 1998; Wolfe et al., 1998) are warmer than those from the early Eocene. General circulation model simulations of the early Eocene using the National Center for Atmospheric Research Community Atmosphere Model (CAM1.4) and atmospheric CO_2 concentrations of 2240 and 4480 ppm simulate mean annual surface air (2 m) temperatures of 23.7 °C and 27.2 °C, respectively, in the Sierra Nevada region (Huber and Caballero, 2011).

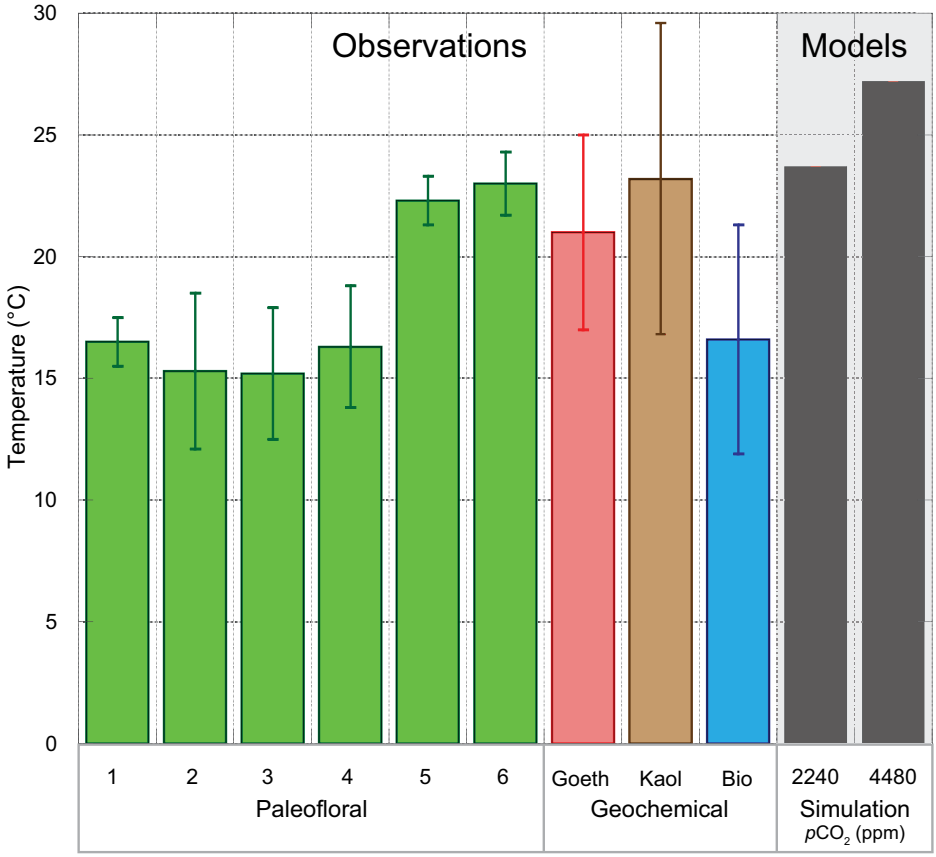

Figure 4. Observed and modeled temperatures of the Eocene Sierra Nevada. Paleofloral estimates: 1—Wolfe (1994), 2–4—Hren et al. (2010), 5—Chase et al. (1998), and 6—Wolfe et al. (1998). Geochemical estimates are from goethite (Yapp, 2008), kaolinite (this study), and biomarker *n*-alkanes (Hren et al., 2010). Eocene climate model simulations are from National Center for Atmospheric Research CAM1.4 with atmospheric pCO_2 of 2240 and 4480 ppm (Huber and Caballero, 2011).

CONCLUSION

Oxygen isotope geochemistry of kaolinites adds robustness to existing hydrogen isotope studies of the Paleogene Sierra Nevada. The oxygen isotope gradient observed in kaolinitized gravels is consistent with orographic rainout of Pacific-derived moisture, and easternmost localities indicate elevations at least as high as 2400 m by the early Eocene. These paleoaltimetry estimates support geomorphic models calling for a trellised drainage network and conflict with tectonic models calling for significant uplift of the northern Sierra Nevada during the late Cenozoic. Kaolinite geothermometry indicates early Eocene weathering occurred between 13.0 °C and 37.2 °C, in agreement with existing paleofloral and geochemical constraints of Eocene climatic temperatures. These temperatures further support the argument that authigenic kaolinites reflect near-surface conditions. Both the growing number and robustness of stable isotope reconstructions contribute to the convergent view of a hot and high Eocene northern Sierra Nevada.

ACKNOWLEDGMENTS

This research was supported by National Science Foundation grants EAR-0309011 and EAR-1019648. Andreas Mulch acknowledges support through the LOEWE funding program of Hesse's Ministry of Higher Education, Research, and the Arts. We thank Michael Hren and two anonymous reviewers for thoughtful comments that greatly improved this paper. We thank Peter Blisniuk for laboratory assistance, Andrea Ritch for helping compile modern water isotope data, Matthew Winnick and Jeremy Caves for helpful discussions, and Kate Maher, Dennis Bird, and Daniel Naylor for productive conversations on weathering reactions and clay isotope systematics.

REFERENCES CITED

Benson, L.V., and White, J.W.C., 1994, Stable isotopes of oxygen and hydrogen in the Truckee River–Pyramid Lake surface-water system. 3. Source of water vapor overlying Pyramid Lake: Limnology and Oceanography, v. 39, p. 1945–1958, doi:10.4319/lo.1994.39.8.1945.

Berger, A., Gnos, E., Schreurs, G., Fernandez, A., and Rakotondrazafy, M., 2006, Late Neoproterozoic, Ordovician and Carboniferous events recorded in monazites from southern-central Madagascar: Precambrian Research, v. 144, p. 278–296, doi:10.1016/j.precamres.2005.11.010.

Bice, K.L., and Marotzke, J., 2001, Numerical evidence against reversed thermohaline circulation in the warm Paleocene/Eocene ocean: Journal of Geophysical Research–Oceans (1978–2012), v. 106, p. 11,529–11,542.

Blisniuk, P.M., and Stern, L.A., 2002, Stable isotope composition of precipitation across the southern Patagonian Andes: Journal of Geophysical Research, v. 107, p. 1–14.

Blisniuk, P.M., and Stern, L.A., 2005, Stable isotope paleoaltimetry: A critical review: American Journal of Science, v. 305, p. 1033–1074, doi:10.2475/ajs.305.10.1033.

Campani, M., Mulch, A., Kempf, O., Schlunegger, F., and Mancktelow, N., 2012, Miocene paleotopography of the central Alps: Earth and Planetary Science Letters, v. 337–338, p. 174–185, doi:10.1016/j.epsl.2012.05.017.

Canavan, R.R., Carrapa, B., Clementz, M.T., Quade, J., DeCelles, P.G., and Schoenbohm, L.M., 2014, Early Cenozoic uplift of the Puna Plateau, Central Andes, based on stable isotope paleoaltimetry of hydrated volcanic glass: Geology, v. 42, p. 447–450, doi:10.1130/G35239.1.

Cassel, E.J., and Graham, S.A., 2011, Paleovalley morphology and fluvial system evolution of Eocene–Oligocene sediments ("auriferous gravels"), northern Sierra Nevada, California: Implications for climate, tectonics, and topography: Geological Society of America Bulletin, v. 123, p. 1699–1719, doi:10.1130/B30356.1.

Cassel, E.J., Graham, S.A., and Chamberlain, C.P., 2009, Cenozoic tectonic and topographic evolution of the northern Sierra Nevada, California, through stable isotope paleoaltimetry in volcanic glass: Geology, v. 37, p. 547–550, doi:10.1130/G25572A.1.

Cassel, E.J., Graham, S.A., Chamberlain, C.P., and Henry, C.D., 2012, Early Cenozoic topography, morphology, and tectonics of the northern Sierra Nevada and western Basin and Range: Geosphere, v. 8, p. 229–249, doi:10.1130/GES00671.1.

Cassel, E.J., Breecker, D.O., Henry, C.D., Larson, T.E., and Stockli, D.F., 2014, Profile of a paleo-orogen: High topography across the present-day Basin and Range from 40 to 23 Ma: Geology, v. 42, p. 1007–1010, doi:10.1130/G35924.1.

Cecil, M.R., Ducea, M.N., Reiners, P.W., and Chase, C.G., 2006, Cenozoic exhumation of the northern Sierra Nevada, California, from (U-Th)/He thermochronology: Geological Society of America Bulletin, v. 118, p. 1481–1488, doi:10.1130/B25876.1.

Chamberlain, C.P., and Poage, M.A., 2000, Reconstructing the paleotopography of mountain belts from the isotopic composition of authigenic minerals: Geology, v. 28, p. 115–118, doi:10.1130/0091-7613(2000)28<115:RTPOMB>2.0.CO;2.

Chamberlain, C.P., Poage, M.A., Craw, D., and Reynolds, R.C., 1999, Topographic development of the Southern Alps recorded by the isotopic composition of authigenic clay minerals, South Island, New Zealand: Chemical Geology, v. 155, p. 279–294, doi:10.1016/S0009-2541(98)00165-X.

Chamberlain, C.P., Mix, H.T., Mulch, A., Hren, M.T., Kent-Corson, M.L., Davis, S.J., Horton, T.W., and Graham, S.A., 2012, The Cenozoic climatic and topographic evolution of the western North American Cordillera: American Journal of Science, v. 312, p. 213–262, doi:10.2475/02.2012.05.

Chamberlain, C.P., Winnick, M.J., Mix, H.T., Chamberlain, S.D., and Maher, K., 2014, The impact of neogene grassland expansion and aridification on the isotopic composition of continental precipitation: Global Biogeochemical Cycles, 2014GB004822, doi:10.1002/2014GB004822.

Chase, C.G., Gregory-Wodzicki, K.M., Parrish-Jones, J.T., and DeCelles, P.G., 1998, Topographic history of the western Cordillera of North America and controls on climate, *in* Crowley, T.J., and Burke, K., eds., Tectonic Boundary Conditions for Climate Model Simulations: New York, Oxford University Press, p. 73–99.

Clark, M.K., 2007, The significance of paleotopography: Reviews in Mineralogy and Geochemistry, v. 66, p. 1–21, doi:10.2138/rmg.2007.66.1.

Clark, M.K., Maheo, G., Saleeby, J., and Farley, K.A., 2005, The non-equilibrium landscape of the southern Sierra Nevada, California: GSA Today, v. 15, no. 9, p. 4–10, doi:10.1130/1052-5173(2005)015[4:TNLOTS]2.0.CO;2.

Craig, H., 1961, Isotopic variations in meteoric waters: Science, v. 133, p. 1702–1703, doi:10.1126/science.133.3465.1702.

Crowley, B.E., Koch, P.L., and Davis, E.B., 2008, Stable isotope constraints on the elevation history of the Sierra Nevada Mountains, California: Geological Society of America Bulletin, v. 120, p. 588–598, doi:10.1130/B26254.1.

DeGraaff-Surpless, K., Graham, S.A., Wooden, J.L., and McWilliams, M.O., 2002, Detrital zircon provenance analysis of the Great Valley Group, California: Evolution of an arc-forearc system: Geological Society of America Bulletin, v. 114, p. 1564–1580, doi:10.1130/0016-7606(2002)114<1564:DZPAOT>2.0.CO;2.

Delgado, A., and Reyes, E., 1996, Oxygen and hydrogen isotope compositions in clay minerals: A potential single-mineral geothermometer: Geochimica et Cosmochimica Acta, v. 60, p. 4285–4289, doi:10.1016/S0016-7037(96)00260-8.

Ducea, M., and Saleeby, J., 1998, Crustal recycling beneath continental arcs: Silica-rich glass inclusions in ultramafic xenoliths from the Sierra Nevada, California: Earth and Planetary Science Letters, v. 156, p. 101–116, doi:10.1016/S0012-821X(98)00021-1.

Feng, R., Poulsen, C.J., Werner, M., Chamberlain, C.P., Mix, H.T., and Mulch, A., 2013, Early Cenozoic evolution of topography, climate, and stable isotopes in precipitation in the North American Cordillera: American Journal of Science, v. 313, p. 613–648, doi:10.2475/07.2013.01.

Frassetto, A.M., Zandt, G., Gilbert, H., Owens, T.J., and Jones, C.H., 2011, Structure of the Sierra Nevada from receiver functions and implications for lithospheric foundering: Geosphere, v. 7, p. 898–921, doi:10.1130/GES00570.1.

Friedman, I., and Smith, G.I., 1970, Deuterium content of snow cores from Sierra Nevada area: Science, v. 169, p. 467–470, doi:10.1126/science.169.3944.467.

Friedman, I., Smith, G.I., Gleason, J.D., Warden, A., and Harris, J.M., 1992, Stable isotope composition of waters in southeastern California 1. Modern precipitation: Journal of Geophysical Research–Atmospheres (1984–2012), v. 97, p. 5795–5812.

Friedman, I., Gleason, J., Sheppard, R.A., and Gude, A.J., 3rd, 1993, Deuterium fractionation as water diffuses into silicic volcanic ash, *in* Union, A.G., ed., Climate Change in Continental Isotopic Records: American Geophysical Union Geophysical Monograph 78, p. 321–323, doi:10.1029/GM078p0321.

Gabet, E.J., 2014, Late Cenozoic uplift of the Sierra Nevada, California? A critical analysis of the geomorphic evidence: American Journal of Science, v. 314, p. 1224–1257, doi:10.2475/08.2014.03.

Galewsky, J., 2009, Orographic precipitation isotopic ratios in stratified atmospheric flows: Implications for paleoelevation studies: Geology, v. 37, p. 791–794, doi:10.1130/g30008a.1.

Garside, L., Henry, C.D., Faulds, J.E., and Hinz, N.H., 2005, The upper reaches of the Sierra Nevada auriferous gold channels, California and Nevada, *in* Proceedings, Symposium 2005: Window to the World: Reno, Nevada, Geological Society of Nevada, p. 209–235.

Garzione, C.N., Dettman, D.L., Quade, J., DeCelles, P.G., and Butler, R.F., 2000, High times on the Tibetan Plateau: Paleoelevation of the Thakkola graben, Nepal: Geology, v. 28, p. 339–342, doi:10.1130/0091-7613(2000)28<339:HTOTTP>2.0.CO;2.

Garzione, C.N., Molnar, P., Libarkin, J.C., and McFadden, B.J., 2006, Rapid late Miocene rise of the Bolivian Altiplano: Evidence for removal of mantle lithosphere: Earth and Planetary Science Letters, v. 241, p. 543–556, doi:10.1016/j.epsl.2005.11.026.

Garzione, C.N., Hoke, G.D., Libarkin, J.C., Withers, S., MacFadden, B., Eiler, J., Ghosh, P., and Mulch, A., 2008, Rise of the Andes: Science, v. 320, p. 1304–1307, doi:10.1126/science.1148615.

Gat, J.R., and Matsui, E., 1991, Atmospheric water balance in the Amazon Basin: An isotopic evapotranspiration model: Journal of Geophysical Research, v. 96, p. 13,179– 13,188, doi:10.1029/91JD00054.

Gébelin, A., Mulch, A., Teyssier, C., Jessup, M.J., Law, R.D., and Brunel, M., 2013, The Miocene elevation of Mount Everest: Geology, v. 41, p. 799–802, doi:10.1130/G34331.1.

Gilbert, H., Yang, Y., Forsyth, D.W., Jones, C.H., Owens, T.J., Zandt, G., and Stachnik, J.C., 2012, Imaging lithospheric foundering in the structure of the Sierra Nevada: Geosphere, v. 8, p. 1310–1330, doi:10.1130/GES00790.1.

Gilg, H.A., Hall, A.M., Ebert, K., and Fallick, A.E., 2013, Cool kaolins in Finland: Palaeogeography, Palaeoclimatology, Palaeoecology, v. 392, p. 454, doi:10.1016/j.palaeo.2013.09.030.

Halevy, I., Fischer, W.W., and Eiler, J.M., 2011, Carbonates in the Martian meteorite Allan Hills 84001 formed at 18 ± 4 °C in a near-surface aqueous environment: Proceedings of the National Academy of Sciences of the United States of America, v. 108, p. 16,895–16,899, doi:10.1073/pnas.1109444108.

Herold, N., Buzan, J., Seton, M., Goldner, A., Green, J.A.M., Müller, R.D., Markwick, P., and Huber, M., 2014, A suite of early Eocene (~55 Ma) climate model boundary conditions: Geoscientific Model Development Discussions, v. 7, p. 529–562, doi:10.5194/gmdd-7-529-2014.

Hetzel, R., Zwingmann, H., Mulch, A., Gessner, K., Akal, C., Hampel, A., Güngör, T., Petschick, R., Mikes, T., and Wedin, F., 2013, Spatiotemporal evolution of brittle normal faulting and fluid infiltration in detachment fault systems: A case study from the Menderes Massif, western Turkey: Tectonics, v. 32, p. 364–376, doi:10.1002/tect.20031.

Horita, J., 1990, Stable isotope paleoclimatology of brine inclusions in halite: Modeling and application to Searles Lake, California: Geochimica et Cosmochimica Acta, v. 54, p. 2059–2073, doi:10.1016/0016-7037(90)90271-L.

Horton, T.W., and Chamberlain, C.P., 2006, Stable isotopic evidence for Neogene surface downdrop in the central Basin and Range Province: Geological Society of America Bulletin, v. 118, p. 475–490, doi:10.1130/B25808.

Horton, T.W., Sjostrom, D.J., Abruzzese, M.J., Poage, M.A., Waldbauer, J.R., Hren, M., Wooden, J., and Chamberlain, C.P., 2004, Spatial and temporal variation of Cenozoic surface elevation in the Great Basin and Sierra Nevada: American Journal of Science, v. 304, p. 862–888, doi:10.2475/ajs.304.10.862.

House, M.A., Wernicke, B.P., and Farley, K.A., 1998, Dating topography of the Sierra Nevada, California, using apatite (U/Th)/He ages: Nature, v. 396, p. 66–69, doi:10.1038/23926.

Hren, M.T., Pagani, M., Erwin, D.M., and Brandon, M., 2010, Biomarker reconstruction of the early Eocene paleotopography and paleoclimate of the northern Sierra Nevada: Geology, v. 38, p. 7–10, doi:10.1130/G30215.1.

Hsieh, J.C.C., and Yapp, C.J., 1999, Stable carbon isotope budget of CO_2 in a wet, modern soil as inferred from $Fe(CO_3)OH$ in pedogenic goethite: Possible role of calcite dissolution: Geochimica et Cosmochimica Acta, v. 63, p. 767–783, doi:10.1016/S0016-7037(99)00062-9.

Huber, M., and Caballero, R., 2003, Eocene El Niño: Evidence for robust tropical dynamics in the "hothouse": Science, v. 299, p. 877–881, doi:10.1126/science.1078766.

Huber, M., and Caballero, R., 2011, The early Eocene equable climate problem revisited: Climate of the Past, v. 7, p. 603–633, doi:10.5194/cp-7-603-2011.

Ibarra, D.E., Egger, A.E., Weaver, K.L., Harris, C.R., and Maher, K., 2014, Rise and fall of late Pleistocene pluvial lakes in response to reduced evaporation and precipitation: Evidence from Lake Surprise, California: Geological Society of America Bulletin, v. 126, p. 1387–1415, doi:10.1130/B31014.1.

Ingersoll, R.V., 2012, Composition of modern sand and Cretaceous sandstone derived from the Sierra Nevada, California, USA, with implications for Cenozoic and Mesozoic uplift and dissection: Sedimentary Geology, v. 280, p. 195–207, doi:10.1016/j.sedgeo.2012.03.022.

Ingraham, N.L., and Taylor, B.E., 1989, The effect of snowmelt on the hydrogen isotope ratios of creek discharge in Surprise Valley, California: Journal of Hydrology (Amsterdam), v. 106, p. 233–244, doi:10.1016/0022-1694(89)90074-7.

Ingraham, N.L., and Taylor, B.E., 1991, Light stable isotope systematics of large-scale hydrologic regimes in Cali-

fornia and Nevada: Water Resources Research, v. 27, p. 77–90, doi:10.1029/90WR01708.

Jeong, G.Y., 1998, Formation of vermicular kaolinite from halloysite aggregates in the weathering of plagioclase: Clays and Clay Minerals, v. 46, p. 270–279, doi:10.1346/CCMN.1998.0460306.

Johnstone, J.A., and Dawson, T.E., 2010, Climatic context and ecological implications of summer fog decline in the coast redwood region: Proceedings of the National Academy of Sciences of the United States of America, v. 107, p. 4533–4538, doi:10.1073/pnas.0915062107.

Joussein, E., Petit, S., Churchman, J., Theng, B., Righi, D., and Delvaux, B., 2005, Halloysite clay minerals—A review: Clay Minerals, v. 40, p. 383–426, doi:10.1180/0009855054040180.

Lawrence, J.R., and Taylor, H.P., 1971, Deuterium and O-18 correlation—Clay minerals and hydroxides in Quaternary soils compared to meteoric waters: Geochimica et Cosmochimica Acta, v. 35, p. 993–1003, doi:10.1016/0016-7037(71)90017-2.

Lechler, A.R., and Galewsky, J., 2013, Refining paleoaltimetry reconstructions of the Sierra Nevada, California, using air parcel trajectories: Geology, v. 41, p. 259–262, doi:10.1130/G33553.1.

Lechler, A.R., and Niemi, N.A., 2011, Sedimentologic and isotopic constraints on the Paleogene paleogeography and paleotopography of the southern Sierra Nevada, California: Geology, v. 39, p. 379–382, doi:10.1130/G31535.1.

Levandowski, W., Jones, C.H., Reeg, H., Frassetto, A., Gilbert, H., Zandt, G., and Owens, T.J., 2013, Seismological estimates of means of isostatic support of the Sierra Nevada: Geosphere, v. 9, p. 1552–1561, doi:10.1130/GES00905.1.

Longstaffe, F.J., and Ayalon, A., 1990, Hydrogen-isotope geochemistry of diagenetic clay minerals from Cretaceous sandstones, Alberta, Canada: Evidence for exchange: Applied Geochemistry, v. 5, p. 657–668, doi:10.1016/0883-2927(90)90063-B.

Lunt, D.J., Dunkley Jones, T., Heinemann, M., Huber, M., LeGrande, A., Winguth, A., Loptson, C., Marotzke, J., Roberts, C.D., Tindall, J., Valdes, P., and Winguth, C., 2012, A model–data comparison for a multi-model ensemble of early Eocene atmosphere–ocean simulations: EoMIP: Climate of the Past, v. 8, p. 1717–1736, doi:10.5194/cp-8-1717-2012.

Ma, L., Castro, M.C., Hall, C.M., and Walter, L.M., 2005, Cross-formational flow and salinity sources inferred from a combined study of helium concentrations, isotopic ratios, and major elements in the Marshall aquifer, southern Michigan: Geochemistry Geophysics Geosystems, v. 6, p. Q10004, doi:10.1029/2005GC001010.

Maher, K., Wooden, J.L., Paces, J.B., and Miller, D.M., 2007, ^{230}Th-U dating of surficial deposits using the ion microprobe (SHRIMP-RG): A microstratigraphic perspective: Quaternary International, v. 166, p. 15–28, doi:10.1016/j.quaint.2007.01.003.

McPhillips, D., and Brandon, M.T., 2012, Topographic evolution of the Sierra Nevada measured directly by inversion of low-temperature thermochronology: American Journal of Science, v. 312, p. 90–116, doi:10.2475/02.2012.02.

Meyer, H.W., 1992, Lapse rates and other variables applied to estimating paleoaltitudes from fossil floras: Palaeogeography, Palaeoclimatology, Palaeoecology, v. 99, p. 71–99, doi:10.1016/0031-0182(92)90008-S.

Minder, J.R., Mote, P.W., and Lundquist, J.D., 2010, Surface temperature lapse rates over complex terrain: Lessons from the Cascade Mountains: Journal of Geophysical Research, ser. D, Atmospheres, v. 115, doi:10.1029/2009JD013493.

Mix, H.T., and Chamberlain, C.P., 2014, Stable isotope records of hydrologic change and paleotemperature from smectite in Cenozoic western North America: Geochimica et Cosmochimica Acta, v. 141, p. 532–546, doi:10.1016/j.gca.2014.07.008.

Mix, H.T., Mulch, A., Kent-Corson, M.L., and Chamberlain, C.P., 2011, Cenozoic migration of topography in the North American Cordillera: Geology, v. 39, p. 87–90, doi:10.1130/G31450.1.

Mix, H.T., Winnick, M.J., Mulch, A., and Chamberlain, C.P., 2013, Grassland expansion as an instrument of hydrologic change in Neogene western North America: Earth and Planetary Science Letters, v. 377–378, p. 73–83, doi:10.1016/j.epsl.2013.07.032.

Molnar, P., 2010, Deuterium and oxygen isotopes, paleoelevations of the Sierra Nevada, and Cenozoic climate: Geological Society of America Bulletin, v. 122, p. 1106–1115, doi:10.1130/B30001.1.

Mulch, A., and Chamberlain, C.P., 2007, Stable isotope paleoaltimetry in orogenic belts—The silicate record in surface and crustal geological archives: Reviews in Mineralogy and Geochemistry, v. 66, p. 89–118, doi:10.2138/rmg.2007.66.4.

Mulch, A., Teyssier, C., Cosca, M.A., Vanderhaeghe, O., and Vennemann, T.W., 2004, Reconstructing paleoelevation in eroded orogens: Geology, v. 32, p. 525–528, doi:10.1130/G20394.1.

Mulch, A., Graham, S.A., and Chamberlain, C.P., 2006, Hydrogen isotopes in Eocene river gravels and paleoelevation of the Sierra Nevada: Science, v. 313, p. 87–89, doi:10.1126/science.1125986.

Mulch, A., Sarna-Wojcicki, A.M., Perkins, M.E., and Chamberlain, C.P., 2008, A Miocene to Pleistocene climate and elevation record of the Sierra Nevada (California): Proceedings of the National Academy of Sciences of the United States of America, v. 105, p. 6819–6824, doi:10.1073/pnas.0708811105.

Mulch, A., Uba, C.E., Strecker, M.R., Schoenberg, R., and Chamberlain, C.P., 2010, Late Miocene climate variability and surface elevation in the Central Andes: Earth and Planetary Science Letters, v. 290, p. 173–182, doi:10.1016/j.epsl.2009.12.019.

Oerter, E., Finstad, K., Schaefer, J., Goldsmith, G.R., Dawson, T., and Amundson, R., 2014, Oxygen isotope fractionation effects in soil water via interaction with cations (Mg, Ca, K, Na) adsorbed to phyllosilicate clay minerals: Journal of Hydrology (Amsterdam), v. 515, p. 1–9, doi:10.1016/j.jhydrol.2014.04.029.

O'Neil, J.R., and Kharaka, Y.K., 1976, Hydrogen and oxygen isotope exchange reactions between clay minerals and water: Geochimica et Cosmochimica Acta, v. 40, p. 241–246, doi:10.1016/0016-7037(76)90181-2.

Oster, J.L., Montañez, I.P., and Kelley, N.P., 2012, Response of a modern cave system to large seasonal precipitation variability: Geochimica et Cosmochimica Acta, v. 91, p. 92–108, doi:10.1016/j.gca.2012.05.027.

Pelletier, J.D., 2007, Numerical modeling of the Cenozoic geomorphic evolution of the southern Sierra Nevada, California: Earth and Planetary Science Letters, v. 259, p. 85–96, doi:10.1016/j.epsl.2007.04.030.

Poage, M.A., and Chamberlain, C.P., 2002, Stable isotopic evidence for a pre–middle Miocene rain shadow in the western Basin and Range: Implications for the paleotopography of the Sierra Nevada: Tectonics, v. 21, p. 16-1–16-10, doi:10.1029/2001TC001303.

Poulsen, C.J., and Jeffery, M.L., 2011, Climate change imprinting on stable isotopic compositions of high-elevation meteoric water cloaks past surface elevations of major orogens: Geology, v. 39, p. 595–598, doi:10.1130/G32052.1.

Renac, C., and Assassi, F., 2009, Formation of non-expandable 7Å halloysite during Eocene–Miocene continental weathering at Djebel Debbagh, Algeria: A geochemical and stable-isotope study: Sedimentary Geology, v. 217, p. 140–153, doi:10.1016/j.sedgeo.2009.04.001.

Rowley, D.B., and Currie, B.S., 2006, Palaeo-altimetry of the late Eocene to Miocene Lunpola basin, central Tibet: Nature, v. 439, p. 677–681, doi:10.1038/nature04506.

Rowley, D.B., and Garzione, C.N., 2007, Stable isotope–based paleoaltimetry: Annual Review of Earth and Planetary Sciences, v. 35, p. 463–508, doi:10.1146/annurev.earth.35.031306.140155.

Rowley, D.B., Pierrehumbert, R.T., and Currie, B.S., 2001, A new approach to stable isotope–based paleoaltimetry: Implications for paleoaltimetry and paleohypsometry of the High Himalaya since the late Miocene: Earth and Planetary Science Letters, v. 188, p. 253–268, doi:10.1016/S0012-821X(01)00324-7.

Rozanski, K., Araguas-Araguas, L., Gonfiantini, R., Swart, P.K., Lohwan, K.L., McKenzie, J.A., and Savine, S., 1993, Isotopic patterns in modern global precipitation, *in* Climate change in continental isotopic records: Washington, DC, American Geophysical Union, p. 1–37.

Rugenstein, M., Stocchi, P., von der Heydt, A., Dijkstra, H., and Brinkhuis, H., 2014, Emplacement of Antarctic ice sheet mass affects circumpolar ocean flow: Global and Planetary Change, v. 118, p. 16–24, doi:10.1016/j.gloplacha.2014.03.011.

Saleeby, J., Ducea, M., and Clemens-Knott, D., 2003, Production and loss of high-density batholithic root, southern Sierra Nevada, California: Tectonics, v. 22, p. 1064, doi:10.1029/2002TC001374.

Savin, S.M., and Epstein, S., 1970, The oxygen and hydrogen isotope geochemistry of clay minerals: Geochimica et Cosmochimica Acta, v. 34, p. 25–42, doi:10.1016/0016-7037(70)90149-3.

Savin, S.M., and Hsieh, J.C.C., 1998, The hydrogen and oxygen isotope geochemistry of pedogenic clay minerals: Principles and theoretical background: Geoderma, v. 82, p. 227–253, doi:10.1016/S0016-7061(97)00103-1.

Saylor, J.E., and Horton, B.K., 2014, Nonuniform surface uplift of the Andean Plateau revealed by deuterium isotopes in Miocene volcanic glass from southern Peru: Earth and Planetary Science Letters, v. 387, p. 120–131, doi:10.1016/j.epsl.2013.11.015.

Sewall, J.O., Sloan, L.C., Huber, M., and Wing, S.L., 2000, Climate sensitivity to changes in land surface characteristics: Global and Planetary Change, v. 26, p. 445–465, doi:10.1016/S0921-8181(00)00056-4.

Sharp, Z.D., 1990, A laser-based microanalytical method for the in situ determination of oxygen isotope ratios of silicates and oxides: Geochimica et Cosmochimica Acta, v. 54, p. 1353–1357, doi:10.1016/0016-7037(90)90160-M.

Sheppard, S.M.F., and Gilg, H.A., 1996, Stable isotope geochemistry of clay minerals: Clay Minerals, v. 31, p. 1–24, doi:10.1180/claymin.1996.031.1.01.

Sieffermann, G., and Millot, 1969, Equatorial and tropical weathering of Recent basalts from Cameron: Allophane, halloysite, metahalloysite, kaolinite and gibbsite: Proceedings of the International Clay Conference, v. 1, p. 417–430.

Sjostrom, D.J., Hren, M., Horton, T.W., Waldbauer, J.R., and Chamberlain, C.P., 2006, Stable isotopic evidence for a pre–late Miocene elevation gradient in the Great Plains–Rocky Mountain region, USA, *in* Willett, S.D., Hovius, N., Brandon, M.T., and Fisher, D.M., eds., Tectonics, Climate, and Landscape Evolution: Geological Society of America Special Paper 398, p. 309–319.

Smith, G.I., Friedman, I., Klieforth, H., and Hardcastle, K., 1979, Areal distribution of deuterium in eastern California precipitation, 1968–1969: Journal of Applied Meteorology, v. 18, p. 172–188, doi:10.1175/1520-0450(1979)018<0172:ADODIE>2.0.CO;2.

Steefel, C.I., and Van Cappellen, P., 1990, A new kinetic approach to modeling water-rock interaction: The role of nucleation, precursors, and Ostwald ripening: Geochimica et Cosmochimica Acta, v. 54, p. 2657–2677, doi:10.1016/0016-7037(90)90003-4.

Stern, L.A., Chamberlain, C.P., Reynolds, R.C., and Johnson, G.D., 1997, Oxygen isotope evidence of climate change from pedogenic clay minerals in the Himalayan molasse: Geochimica et Cosmochimica Acta, v. 61, p. 731–744, doi:10.1016/S0016-7037(96)00367-5.

Stock, G.M., Anderson, R.S., and Finkel, R.C., 2004, Pace of landscape evolution in the Sierra Nevada, California, revealed by cosmogenic dating of cave sediments: Geology, v. 32, p. 193–196, doi:10.1130/G20197.1.

Stock, G.M., Anderson, R.S., and Finkel, R.C., 2005, Rates of erosion and topographic evolution of the Sierra Nevada, California, inferred from cosmogenic ^{26}Al and ^{10}Be concentrations: Earth Surface Processes and Landforms, v. 30, p. 985–1006, doi:10.1002/esp.1258.

Tabor, N.J., and Montañez, I.P., 2005, Oxygen and hydrogen isotope compositions of Permian pedogenic phyllosilicates: Development of modern surface domain arrays and implications for paleotemperature reconstructions: Palaeogeography, Palaeoclimatology, Palaeoecology, v. 223, p. 127–146, doi:10.1016/j.palaeo.2005.04.009.

Takeuchi, A., and Larson, P.B., 2005, Oxygen isotope evidence for the late Cenozoic development of an oro-

graphic rain shadow in eastern Washington, USA: Geology, v. 33, p. 313–316, doi:10.1130/G21335.1.

Unruh, J.R., 1991, The uplift of the Sierra Nevada and implications for late Cenozoic epeirogeny in the western Cordillera: Geological Society of America Bulletin, v. 103, p. 1395–1404, doi:10.1130/0016-7606(1991)103<1395:TUOTSN>2.3.CO;2.

Van Buer, N.J., Miller, E.L., and Dumitru, T.A., 2009, Early Tertiary paleogeologic map of the northern Sierra Nevada batholith and the northwestern Basin and Range: Geology, v. 37, p. 371–374, doi:10.1130/G25448A.1.

Vitali, F., Longstaffe, F.J., McCarthy, P.J., Plint, A.G., and Caldwell, W.G.E., 2002, Stable isotopic investigation of clay minerals and pedogenesis in an interfluve paleosol from the Cenomanian Dunvegan Formation, N.E. British Columbia, Canada: Chemical Geology, v. 192, p. 269–287, doi:10.1016/S0009-2541(02)00225-5.

Wakabayashi, J., 2013, Paleochannels, stream incision, erosion, topographic evolution, and alternative explanations of paleoaltimetry, Sierra Nevada, California: Geosphere, v. 9, p. 191–215, doi:10.1130/GES00814.1.

Wakabayashi, J., and Sawyer, T.L., 2001, Stream incision, tectonics, uplift, and evolution of topography of the Sierra Nevada, California: The Journal of Geology, v. 109, p. 539–562, doi:10.1086/321962.

Wernicke, B., and 18 others, 1996, Origin of high mountains in the continents: The southern Sierra Nevada: Science, v. 271, p. 190–193, doi:10.1126/science.271.5246.190.

Winnick, M.J., Chamberlain, C.P., Caves, J.K., and Welker, J.M., 2014, Quantifying the isotopic "continental effect": Earth and Planetary Science Letters, v. 406, p. 123–133, doi:10.1016/j.epsl.2014.09.005.

Wolfe, J.A., 1994, Tertiary climatic changes at middle latitudes of western North America: Palaeogeography, Palaeoclimatology, Palaeoecology, v. 108, p. 195–205, doi:10.1016/0031-0182(94)90233-X.

Wolfe, J.A., Forest, C.E., and Molnar, P., 1998, Paleobotanical evidence of Eocene and Oligocene paleoaltitudes in midlatitude western North America: Geological Society of America Bulletin, v. 110, p. 664–678, doi:10.1130/0016-7606(1998)110<0664:PEOEAO>2.3.CO;2.

Yapp, C.J., 2008, $^{18}O/^{16}O$ and D/H in goethite from a North American Oxisol of the early Eocene climatic optimum: Geochimica et Cosmochimica Acta, v. 72, p. 5838–5851, doi:10.1016/j.gca.2008.09.002.

Zandt, G., Gilbert, H., Owens, T.J., Ducea, M., Saleeby, J., and Jones, C.H., 2004, Active foundering of a continental arc root beneath the southern Sierra Nevada in California: Nature, v. 431, p. 41–46, doi:10.1038/nature02847.

Ziegler, K., Hsieh, J.C.C., Chadwick, O.A., Kelly, E.F., Hendricks, D.M., and Savine, S.M., 2003, Halloysite as a kinetically controlled end product of arid-zone basalt weathering: Chemical Geology, v. 202, p. 461–478, doi:10.1016/j.chemgeo.2002.06.001.

Science Editor: David Ian Schofield
Associate Editor: Benjamin J.C. Laabs

Manuscript Received 3 February 2015
Revised Manuscript Received 14 July 2015
Manuscript Accepted 9 September 2015

Printed in the USA

Geological Society of America Bulletin

A hot and high Eocene Sierra Nevada

Hari T. Mix, Daniel E. Ibarra, Andreas Mulch, Stephan A. Graham and C. Page Chamberlain

Geological Society of America Bulletin published online 21 October 2015;
doi: 10.1130/B31294.1